Mediterranean sea level variations: Analysis of the satellite altimetric data, 1992-2008

M.I. Vigo, J.M. Sanchez-Reales, M. Trottini, B.F. Chao

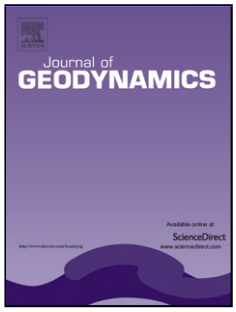

Title: Mediterranean sea level variations: Analysis of the satellite altimetric data, 1992-2008

Authors: M.I. Vigo, J.M. Sanchez-Reales, M. Trottini, B.F. Chao

PII: S0264-3707(11)00029-9
DOI: doi:10.1016/j.jog.2011.02.002
Reference: GEOD 1045

To appear in: *Journal of Geodynamics*

Received date: 13-10-2010
Revised date: 1-2-2011
Accepted date: 1-2-2011

Please cite this article as: Vigo, M.I., Sanchez-Reales, J.M., Trottini, M., Chao, B.F., Mediterranean sea level variations: Analysis of the satellite altimetric data, 1992-2008, *Journal of Geodynamics* (2010), doi:10.1016/j.jog.2011.02.002

Mediterranean sea level variations: Analysis of the satellite altimetric data, 1992-2008

M. I. Vigo[(1)], J. M. Sanchez-Reales[(1)], M. Trottini[(2)], and B. F. Chao[(3)].

(1) Department of Applied Mathematics,
University of Alicante,
Alicante, E03080, Spain.
Email: vigo@ua.es

(2) Department of Statistics,
University of Alicante,
Alicante, E03080, Spain
Email: mario.trottini@ua.es

(3) Institute of Earth Sciences
Academia Sinica,
Taipei, Taiwan, ROC
E-mail: bfchao@earth.sinica.edu.tw

Abstract

Sixteen years of satellite radar altimeter data are analyzed to investigate the sea-level variation (SLV) of the Mediterranean Sea. The time evolution of the overall mean sea level of the Mediterranean Sea follows its own regional dynamics. The geographical distribution of the seasonal signal (annual and semi-annual) indicates that the major features of the Mediterranean Sea circulation are driving the highest seasonal variability, and that an eastward propagation exists between the western and eastern basins. While in previous studies the trend of SLV has been modeled as linear, in this study with a longer record of observations we found that a quadratic acceleration term is statistically significant for practically the whole basin, especially in those regions where the trend provides a significant contribution to the SLV. The inclusion of the quadratic acceleration term accounts better for the Mediterranean SLV trend, as the residual low frequency SLV in wintertime is highly correlated with NAO at zero time lag in almost the whole basin. The residual high-frequency signal variability, on the other hand, can be explained by mesoscale phenomena, such as eddies and gyres. Our comprehensive analysis of the Mediterranean SLV provides source observations for monitoring and understanding of both regular and transient phenomena.

1. Introduction

The altimetric satellites provide accurate data of the sea level variations (SLV) useful for the modeling and understanding of their complex spatial distribution and temporal evolution. For the Mediterranean Sea, which is the target of the present study, altimetry data have been mainly used to study annual and interannual SLV. Several

studies based on altimetry data for the period 1993-1999 (Cazenave *et al.*, 2001, 2002; Fenoglio-Marc, 2002) indicated a sea level drop in the Ionian Sea and a sea level rise in the rest of the Mediterranean (although less pronounced in the Western basin). In all cases the reported trend is linear during the time period. This pattern was found to be highly correlated with the Sea Surface Temperature (SST) and explained in terms of steric height variations.

Extending the period of study to 2003, Vigo *et al.* (2005) reported a reversal in 1999 of the SLV trend on sub-basin scale, suggesting a change in thermohaline circulation in the eastern Mediterranean, in particular with the ending of the Eastern Mediterranean Transient. Covering the period l993-2005, Criado *et al.*, (2008) confirmed this trend change, and detected a negative trend from 2001 onwards in the thermosteric component of the mean Mediterranean SLV computed from the output temperature profiles of ECCO ocean model (Stammer *et al.*, 2002).

In this work we take a step further in the analysis of the Mediterranean SLV extending the time period to more than 16 years – from October 1992 to December 2008, for which multi-satellite altimetric data are available. SLV is locally modeled as a sum of the seasonal (annual + semiannual) component, a linear trend, plus a quadratic term. We show that the quadratic acceleration as part of decadal fluctuation is statistically significant within the studied time span. We shall analyze the contribution of the North Atlantic Oscillation (NAO) to the interannual SLV of the Mediterranean Sea, complementing previous studies by Woolf *et al.* (2003) and Tsimplis *et al.* (2008). The NAO is the most prominent interannual meteorological fluctuation in the North Atlantic with major impacts on, among others, sea-level in the region especially in the winter (Hurrell, 1995), as studied by Tsimplis and Baker (2000), Tsimplis and Josey

(2001) for the period of the 1960s through the 1990s. We shall also examine the relationship between the residual high-frequency SLV and Mediterranean mesoscale circulation in space and time, and show how a proper modeling of the SLV trend, including the quadratic term, improves the capability of mapping mesoscale phenomena such as eddies and gyres (e.g. Stammer, 1997) or subbasin-wide Eddy Kinetic Energy variability (Pujol and Larnicol, 2005; Pascual et al., 2007).

2. Data and Mean Sea Level

We study the SLV for the Mediterranean Sea with combined data from several altimetric satellites: ERS-1/2, Topex/Poseidon (T/P), ENVISAT, and Jason-1/Jason 2 (see AVISO release, http://www.aviso.oceanobs.com, 2010). These altimetric data are weekly sea level anomalies at 1/8ºx1/8º grids from October 1992 to December 2008 (16 years), with respect to the CLS01 Mean Sea Surface estimated from 7 years of measurements of T/P (1993-1999), 5 years of ERS-1/2 and 2 years of Geosat. State of the art corrections are applied including ionosphere delay, dry and wet tropospheric corrections, electromagnetic bias, solid and ocean tides, ocean tide loading, pole tide, sea state bias, and instrumental corrections. In addition, the so-called dynamic atmospheric correction is included, undoing the high-frequency (<20 days) response of the ocean to atmospheric pressure and winds given by a 2D-model and the low-frequency (>20 days) part of the inverted barometer (IB) ocean response to overlying pressure. Gaps in the data of up to 6 weeks in small areas in the Alboran, North Adriatic and Aegean Seas (less than 1% of the total data) have been linearly interpolated.

Figure 1.a presents the spatial mean of the Mediterranean SLV as a function of time, which clearly indicates a strong seasonal signal composed of annual and semi-annual

terms, as well as interannual variability. The non-seasonal variation, after the seasonality has been subtracted, in Figure 1.b demonstrates how different time periods would have different apparent linear trends. Thus, to better account for possible temporal acceleration/deceleration, the trend will be model as the sum of a linear trend plus a quadratic term that represents acceleration when positive or deceleration when negative. Thus, we model the SLV as the following *quadratic acceleration model*:

$$SLV(t) = A_a \cos(\omega_a t - \phi_a) + A_{sa} \cos(\omega_{sa} t - \phi_{sa}) + B + C(t - \bar{t}) + D(t - \bar{t})^2 + \varepsilon(t) \quad (1)$$

where $\bar{t}$ is the mid-point of the time span, $A_a \cos(\omega_a t - \phi_a)$ accounts for the annual signal, $A_{sa} \cos(\omega_{sa} t - \phi_{sa})$ for the semiannual signal, and $\varepsilon(t)$ is the un-modeled residual term with zero mean. We estimate the parameters in Equation (1) by the least-squares procedure. The least-squares estimate for the annual amplitude is 7 cm with corresponding phase equivalent to 278 days, and the semiannual amplitude is 1.05 cm with 130 days for the phase. As a result the minimum and maximum of the seasonal cycle are reached in middle March and middle October, respectively.

[Figure 1]

Figure 1. (a) Mediterranean mean SLV time series; (b) non-seasonal signal of (a).

The interannual variation (Figure 1.b) can be described as a linear trend of 0.16 cm/year with a slight quadratic acceleration of -0.063 cm/year^2, superimposed to some high frequency signal that are related to wind-driven water flow through the Gibraltar Strait (Fukumori *et al.*, 2007; Garcia *et al.*, 2010).

3. Seasonal SLV

We least-squares fit at each grid location a quadratic model similar to Equation (1). The estimated annual amplitudes and phases "maps" are shown in Figure 2. The amplitudes of the annual cycle (Figure 2.a) vary from 4 to 11 cm, except for a small area of value around 16 cm at the south-east of Crete corresponding to the Ierapetra gyre activity. High variability is also associated with the two gyres in the Alboran Sea corresponding to the two foci of amplitude around 8 and 12 cm, and the Bonifacio Gyre at the southeast of Corsica. On the other hand lower variability is observed in the Gulf of Lion and the eastern basin at the Adriatic and Aegean Seas, where winter cooling produces the deep water in the western and eastern Mediterranean, respectively.

[Figure 2]

Figure 2. Seasonal component of SLV: a) annual amplitude; b) annual phase; c) semiannual amplitude; d) semiannual phase.

The annual phase map (Figure 2.b) shows that the western basin reaches its annual maximum in late September, anticipating the eastern basin by approximately two weeks and the Adriatic by 4 weeks. This pattern evokes the pattern of circulation of the Atlantic water into the Mediterranean Sea as provided by Millot *et al.*, (2005). Thus, it suggests that the redistribution of the Atlantic water influences the annual cycle to a certain extent, reaching the maximum progressively in time depending on the distance from the Gibraltar Strait.

For most of the Mediterranean Sea the semiannual amplitude (Figure 2.c) is small except for isolated pockets where it reaches values close to 3 cm (e.g., south of Peloponnesus peninsula, southeast of Sicily, in the Gulf of Lyon and some location in the Alboran Sea). In terms of the semiannual phase (Figure 2.d), an abrupt phase change

between western and eastern Mediterranean is shown, reaching the latter with maximum in May.

The above seasonal behaviour of the Mediterranean SLV agrees with previous results from altimetry data (Cazenave *et al.*, 2001, Fenoglio *et al.*, 2002, Vigo *et al.*, 2005). It is consistent also with seasonal variability of the Mediterranean circulation as modeled by Rossenov *et al.*(1995). The major features of the Mediterranean Sea circulation are driving the highest seasonal variability.

4. Linear trend and quadratic acceleration in SLV

Limited by the available time span, previous studies of spatially averaged SLV for the Mediterranean reported the estimated linear trend at rates between 7± 1.5 mm/year and 2.1 ± 0.6 mm/year depending on the period of study (e.g., Cazenave *et al.*, 2002; Vigo *et al.*, 2005). Here a longer time span of 16 years of altimetric record allows to detect not only a linear trend but also a quadratic acceleration.

Goodness of fit of the proposed quadratic acceleration model at each location has been measured in terms of *R-squared* which, in our case, represents the proportion of SLV variability explained by the quadratic fit (for a formal definition of *R-squared* and its interpretation as measure of model fit see appendix A). As shown in Figure 3, the proposed model describes quite well the variance of the SLV – the proportion of explained variance exceeds 50% for 86% of the region. Note that the small areas of poor fit (small R-squared) all correspond to well-known areas of mesoscale phenomena (see section 6 and Figure 9.b).

[Figure 3]

Figure 3. R-squared value for the quadratic trend model fitted at each grid location

The use of the quadratic acceleration model raises the question as to whether or not it is worthwhile to include a quadratic acceleration term in modeling SLV. We addressed the statistical significance of the quadratic acceleration term by comparing at each location the SLV variance explained by the quadratic model with the corresponding variance explained by the model without the quadratic term, properly accounting for the number of free parameters in the two models by means of a F-test (see Draper and Smith, section 2.7 page 97). For each location we obtained the value of the statistic for *extra sum of squares*, F, which is a measure of the *extra sum of squares* (explained variance) due to the inclusion of the quadratic acceleration term. A "large" value of the F statistic at a certain location indicates that for that location the extra sum of squares due to the inclusion of the quadratic term is significantly large and the quadratic term should be included in the model. The results are shown in Figure 4.a. It can be observed that for more than the 80% of the region the quadratic acceleration term is statistically significant. This means that at most locations the quadratic model should be preferred over just the linear trend model.

A comparison of the two models can also be performed by comparing the *adjusted R-squared* (see appendix A) of the models at each location. The *adjusted R-square* is also a measure of model fit but includes a penalty for the number of parameters in the model (comparison of the two models based on *R-squared* would be meaningless since *R-squared,* by definition, would always select the more complex model). For a formal definition of *adjusted R-square* and its interpretation as measure of model fit and model comparison see appendix A. Figure 4.b shows the difference at each location between the *adjusted R-squared* values for the two models (with and without the quadratic term). Again, we observe that for most of the locations the adjusted R-squared value for the

quadratic model is greater than that without, favoring the quadratic model, despite the penalty for the larger number of parameters. In particular, the largest gain is for the Ionian Sea and other small regions in the eastern basin. Incidentally, as a simple experiment we tested the analysis adding the 2009 data, and confirmed that cubic terms become significant in addition to quadratic terms, but only for regions where the trend contribution to SLV is negligible (see Figure 5).

[Figure 4]

Figure 4. (a) F test for the statistical significance of the quadratic acceleration term. Locations where the quadratic term is significant at the significant level of 0.05 are in red. (b) Difference between the adjusted R-squared values with and without the quadratic acceleration term.

Figure 5 shows the contribution to the explained SLV variance of the seasonal and the quadratic term. The seasonal contribution is obtained as the ratio of the variance of SLV predicted by the estimated quadratic model to that of SLV predicted by the seasonal component of the estimated quadratic acceleration model. The trend contribution is measured as the difference between the estimated SLV variance and the seasonal contribution. It can be seen that the seasonal component explains most of the estimated SLV variability in areas where the linear trend and quadratic models perform almost equally well. For those regions where the trend provides a significant contribution to the SLV, the linear trend is inferior to a quadratic acceleration.

[Figure 5]

Figure 5. Contribution to the explained SLV variance of: (a) the seasonal component (annual + semiannual), and (b) the trend component of the quadratic acceleration model.

Combining the information in the linear trends and quadratic accelerations maps (shown in Figure 6) we find that, in agreement with Figure 4.b and 5, for most of the Mediterranean region linear and quadratic terms are close to zero and the trend component has a negligible contribution to SLV variability (dark blue area in Figure 5.b). The highest values of acceleration are observed in the Ionian Sea where the (negative) linear trend is also high in absolute value. As a result the trend component in the Ionian is very strong and can be described by a (negative) linear trend with (positive) quadratic acceleration. Large (positive) values for the linear trend are also observed south of the Peloponnesus peninsula where the acceleration term is close to zero.

[Figure 6]

Figure 6. Mediterranean SLV maps of: (a) linear trends, and (b) quadratic accelerations as estimated by the quadratic acceleration model.

The geographical distribution of various trending of SLV in the Mediterranean is given in Figure 7. Except for 13% of the area (in red) of monotonic rising in SLV and small pockets of apparent drop of SLV (in green, 0.6% of area), the majority 68% of the whole region (in blue) sees rising of SLV at the beginning of the period and then drops due to negative acceleration while 19% of the area (in violet) sees SLV drop first followed by a rise giving the positive acceleration.

[Figure 7]

Figure 7. Geographical distribution of various trend curves of SLV observed in the Mediterranean Sea. Four types of trend are observed: convex upward (in violet, SLV

drops first and then rises); convex downward (in blue, SLV first rises and then drops); monotonic increasing (in red); and monotonic decreasing (in green).

Figure 8 shows the distribution of the range of the SLV (in centimeters) in the quadratic trend (i.e. difference between minimum and maximum values of SLV associated with the linear plus quadratic terms) during the study period, and the epoch at which maximum/minimum is reached. Not surprisingly the largest variations are observed in those areas where the contribution of the trend is more significant. For most of the locations the inversion of the SLV trend curves happens between late 1999 and 2003. The latter is in agreement with previous results reported in Vigo *et al.*, (2005), who observed an SLV change in late 1999 from dropping to rising in the Ionian Sea and the opposite in the Levantine, Adriatic and Aegean Basins. There are a few areas where the inversion is observed at the very beginning of the period or at the very end.

[Figure 8]

Figure 8. (a) The distribution of the range of the SLV (in centimeters) in the quadratic trend during the study period; (b) the epoch at which maximum/minimum SLV is reached, for the convex (upward and downward) trends. Areas where the trend is monotonic (increasing or decreasing) are represented in white.

5. Interannual SLV and NAO

North Atlantic Oscillation (NAO) is a leading mode of climatic variability in the Northern oceans through ocean-atmosphere interactions. Several studies have demonstrated the influence of the NAO on the SLV around Europe (Tsimplis and Josey, 2001; Woolf *et al.*, 2003). Over the past several decades NAO has been mostly in the state of strong warming and wetter-than-normal conditions over much of northern

Europe, while colder and drier conditions have prevailed over much of southern Europe and northern Africa (Hurrell, 1995, Hurrell and Deser, 2009). In this section we investigate the relationship of the Mediterranean SLV with NAO, the latter in terms of the NAO Index (NAOI) defined as the time series of the primary mode from a Rotated Principal Component Analysis of the mean standardized 500-mb height anomalies (provided by the Climate Prediction Center of NOAA, http://www.cpc.noaa.gov/data/teledoc/teleindcalc.shtml).

We only concentrate on the extended wintertime from December to March, when NAO influence is the strongest. Figure 9.a compares the NAOI time series (actually the negative of NAOI according to the usual convention) with the mean non-seasonal SLV for the extended wintertime; Figure 9.b presents the cross-correlation function between the two time series as a function of time lag of SLV versus –NAOI.

[Figure 9]

Figure 9. Extended wintertime only: (a) Mean SLV versus –NAOI (zero lag); (b) cross correlation function between mean SLV and –NAOI time series.

The correlation coefficient (at zero time lag) reaches 0.61 and is statistically significant at the significance level 0.01 (p-value < 0.001 with 95% confidence interval [0.43, 0.74] at 62 degrees of freedom). The R-squared is 0.37, which means that after removing the seasonal signal, NAO nominally explains 37% of the mean sea level variance.

Geographical details of the above relationship between NAO and non-seasonal and detrended residual wintertime SLV are given in Figure 10. Figure 10.a shows the zero-lag correlation map. In general, sea level is lower in NAOI positive winters. To describe the influence of NAO on SLV we have regress wintertime residual SLV on –NAOI.

Figure 10.b shows the sensitivity map of SLV to NAO as the regression coefficient for the –NAOI. Note that the influence of NAO progressively increases from west to east over the Mediterranean Sea.

[Figure 10]

Figure 10. Geographical distribution of the correlation between –NAOI and non-seasonal detrended residual SLV: (a) zero-lag correlation map; (b) sensitivity map for the regression of residual SLV on –NAOI.

Comparison of correlation maps of –NAOI with residual SLV separately for the quadratic acceleration model and the linear trend model (maps not shown) indicates that the correlation increases notably when the quadratic term is adopted compared with otherwise.

High correlation of NAO with non-seasonal Mediterranean SLV was already reported in previous studies but using different observables and for different time periods (e.g., Tsimplis and Josey, 2001; Tsimplis and Shaw, 2008; Woolf et al., 2003). Although the IB correction (the hydrostatic effects of atmospheric pressure loading) has been applied to the data, it is known that significant departures from IB can be observed over restricted seas or basin such as the Mediterranean Sea for periods shorter than 6-10 months (Le Traon and Gauzelin, 1997). Nevertheless, the discrepancy becomes negligible as far as interannual SLV are concerned. The response of the Mediterranean to NAO can be attributed in part to both the southern node of the pressure dipole and to the effect of NAO on surface fluxes (Tsimplis and Baker, 2000; Tsimplis and Josey, 2001; Woolf et al., 2003). SLV in the basin represents a response to changes in the surface pressure associated with the reversal of the NAO state. It has also been linked in

the past to the Eastern Mediterranean Transient (EMT) that occurred between 1987 and 1992 (Klein et al., 2000; Roether et al., 1996), with the change in the freshwater flux in the basin caused by the consistently stronger NAO during the 1990s (Tsimplis and Josey, 2001). The demostrated influence of NAO in the circulation of the northwestern Mediterranean Sea (Vignudelli et al., 1999) establishes the basis of the connection between NAO and the recent changes in both the Mediterranean SLV and thermohaline circulations.

6. Residual high-frequency SLV and EKE

Besides the NAO-related interannual SLV variability, Figure 11.a presents the map of the standard deviation of the high-frequency residual SLV after removal of all the fitted signals above from Equation 1. The generally low residual values mean that the fit does explain most of the SLV signal power, but there remain a few isolated locations showing remaining but significant high-frequency signals, most of which correspond to well-known regions of mesoscale phenomena which play an important role in the formation and spreading of water masses in the Mediterranean Sea (Alhammoud *et al.*, 2005; Demirov and Pinardi, 2006; Millot and Taupier-Letage, 2005). Figure 11.b shows the geographical distribution of the mean Eddy Kinetic Energy (EKE) derived from the geostrophic currents from SLV, as distributed by Aviso:

$$\mathrm{EKE}(t) = 1/2\ [\ U^2(t) + V^2(t)\ ] \qquad (2)$$

where $U(t)$ and $V(t)$ are respectively the meridional and zonal geostrophic velocities as functions of time. This result is in agreement with those discussed in detail in the work by Pujol and Larnicol (2005), where EKE maps were deduced from altimetry data but using the standard deviation of the original SLV as opposed to that of the residual SLV (as we did here) which we argue to be more effective. For example, we found that the

Ionian Sea has very high SLV standard deviations only because of the seasonal and strong trend signals, with almost no accumulation of EKE (see Figure 11.b).

[Figure 11]

Figure 11. (a) Standard deviation of our processed residual SLV; and (b) Mean EKE in the Mediterranean Sea according to AVISO.

Similarity between the two maps in Figure 11 (with spatial correlation of 0.80) evidences that the residual high-frequency SLV variability is mainly driven by the mesoscale oceanic phenomena, such as eddies and gyres. For the period of study, accumulation of eddies are particularly prominent in the west Levantine and the east Algerian subbasins as well as the gyres in the Alboran Sea, and, to a lesser extent, the central Ionian, the east Levantine subbasin, and around the Balearic Islands.

Thus, the eddy evolution in time and space can be studied from the residual SLV. In Figure 12 we show the N-S latitudinal profile along longitude 26.5º E, and the E-W Longitudinal profile along latitude 34.25º N as a function of time, corresponding to the Ierapetra gyre southeast of Crete. The residual SLV at this location fluctuates with amplitudes range more than 60 cm. During 1999 when SLV showed a stable positive anomaly higher than 15 cm, the Ierapetra gyre moved southwest-ward. On the other hand, a notable increase in the size of the gyre can be seen in early 2003 -- after a more or less stable behaviour in 2002 the gyre increased by three-fold its diameter in longitude and doubles in latitude in the first half of 2003.

[Figure 12]

Figure 12. Time profiles of the residual SLV along longitude 26.5º E and latitude 34.25º N.

7. Conclusions

We conduct a comprehensive study of the sea-level variation (SLV) of the Mediterranean Sea using satellite radar altimeter data for the period October 1992-December 2008. We identify the signals in terms of their geographical distribution and temporal evolution, and found that:

(1) After removing the seasonal signal, the temporal trend including the quadratic acceleration of the mean sea level displays an overall increase of 2.6 cm in the study period, peaking at mid-June 2003 by 3.6 cm and then dropping 1 cm from there till the end of 2008. This change is not consistent with the global SLV that has been rising at a rate of 3.0 - 3.5 mm/yr since 1992 (e.g., Ablain *et al.* 2009; Beckley *et al.* 2007, Leuliette *et al.*, 2004). This different behavior indicates that being a semi-enclosed basin the Mediterranean does not respond linearly to the influences of the open ocean on the timescale in question. In fact, previous studies have shown that the mass contribution to the Mediterranean SLV has been decreasing from 2006 (García et al., 2010), despite the increasing mass contribution in the global ocean (Cazenave et al., 2009).

(2) The seasonal component explains most of the SLV variability. The geographical distribution of the annual and semi-annual signals are obtained. The western basin reaches its annual maximum in early autumn, anticipating the eastern basin by two weeks and the Adriatic by 4 weeks. In the semiannual signal an eastward propagation over a span of 80 days exists between the western and eastern basins, the latter reaching maximum in May.

(3) The linear temporal trends and a quadratic acceleration in the SLV are found to be significant in general. Analyzing the statistical contribution of each component of the model we found that despite the fact that for most of the Mediterranean region the seasonal component explains most of the variability, for those regions where the trend provides a significant contribution to the SLV, the long-term trend is subject to a quadratic acceleration. These results are not in general agreement with previous studies where only a linear trend (for a shorter time span) is estimated.

(4) The interannual signal in the mean Mediterranean SLV is highly correlated with NAO with no significant time lag. We have studied the geographical distribution of the correlation between residual SLV (non-seasonal and detrended) and –NAOI at zero lag, and the SLV sensitivity to NAO, finding a statistically significant sensitivity to NAO in almost the whole basin.

(5) The residual high-frequency signals can be explained by mesoscale phenomena, such as eddies and gyres. Our study suggests that a proper modeling of the deterministic component of SLV might provide a useful tool to study the evolution in time and space of mesoscale structures, considering zonal and meridional profiles of residual SLV at the center of the structure of interest.

Acknowledgments

This work was partly funded by the Spanish Ministry of Education and Science under the research project AYA2009-07981, and the Geophysics Program of the National Science Council of Taiwan. Authors would like to acknowledge the AVISO (Archiving

Validation and Interpretation of Satellite Oceanographic data) project for providing the altimetry products used in this analysis.

Appendix A

Consider a linear regression model and suppose that a sample of *n* units has been observed. Let y_i be the value the response variable in the *i-th* individual, $\hat{y}_i$ the corresponding value estimated from the model, and $\bar{y}$ the sample mean for the response variable. Let SST, SSR and SSE be the *total, residual* and *explained* sum of squares,

$$SST = \sum_{i=1}^{n} (y_i - \bar{y})^2; \qquad SSR = \sum_{i=1}^{n} (\hat{y}_i - \bar{y})^2; \qquad SSE = \sum_{i=1}^{n} (y_i - \hat{y}_i)^2$$

The *R-squared* is defined as (see, for example, Montogomery, Peck, and Vining G. G. page 39) :

$$R^2 = 1 - \frac{SSE}{SST} = \frac{SSR}{SST}.$$

The R-squared can be interpreted as a measure of model fit, it represents the proportion of response variation explained by the model. However *R-square* is not suitable for comparing models since addition of independent variables (regressors) to a fitted model will generally increase (and will never decrease) the *R-square* so that complex models would always be preferred to simpler models. This is why in the analysis the comparison of the quadratic and linear model was based on the *adjusted R squared*, defined as (see, for example, Montogomery, Peck, and Vining G. G. page 90):

$$Adjusted\, R^2 = 1 - (1 - R^2) \cdot \frac{n-1}{n-p} = 1 - \frac{SSE}{SST} \cdot \frac{n-1}{n-p} \qquad (3)$$

where *p* is the number of parameters in the model. As shown in (3) the *adjusted R*-square is also a measure of model fit but includes a penalty for the number of parameters in the model. Thus given two nested models the complex model is preferred to the simpler model only if the gain in model fit for adding extra parameters is superior to the penalty for the large number of parameters. As it can be seen in Figure 4.b the difference in adjusted R-squared for the linear and quadratic model is not always positive but can be negative too.

References

Ablain M., Cazenave, A., Guinehut, S. and Valladeau, G., 2009. A new assessment of global mean sea level from altimeters highlights a reduction of global slope from 2005 to 2008 in agreement with in-situ measurements, Ocean Sciences, 5, 193-201.

Alhammoud, B., Beranger, K., Mor tier, L., Crepon, M., and Dekeyser, I., 2005. Surface circulation of the Levantine Basin: comparison of model results with obser vations, Prog. Oceanogr., 66(2–4), 299–320.

Barnston, A. G., and Livezey, R. E., 1987. Classification, seasonality and persistence of low-frequency atmospheric circulation patterns. Mon. Wea. Rev., 115, 1083-1126.

Beckley, B. D., Lemoine, F. G., Luthcke, S. B., Ray, R. D. and Zelensky, N. P., 2007. A reassessment of global rise and regional mean sea level trends from TOPEX and Jason-1 altimetry based on revised reference frame and orbits, Geophys. Res. Lett., 34, L14608, doi:10.1029/2007GL030002.

Cazenave A., Cabanes, C., Dominh, K. and Mangiarotti, S., 2001. Recent sea level change in the Mediterranean sea revealed by satellite altimetry, Geophys. Res. Lett., *28(8)*, 1607-1610.

Cazenavea, A., Dominha, K., Guinehutb, S., Berthiera, E., Llovela, W., Ramilliena, G., Ablainb, M. and Larnicol, G., 2009. Sea level budget over 2003–2008: A

472 reevaluation from GRACE space gravimetry, satellite altimetry and Argo, Global
473 and Planetary Change, *65(1-2)*, 83-88, doi:10.1016/j.gloplacha.2008.10.004
474 Cazenave, A., Bonnefond, P., Mercier, F., Dominh, K. and Toumazou, V., 2002. Sea
475 level variations in the Mediterranean Sea and Black Sea from satellite altimetry and
476 tide gauges. Global and Planetary Change, *34(1-2)*, 59-86
477 Criado Aldeanueva, F. , Del Río Vera and J., and García Lafuente, J., 2008. Steric and
478 mass-induced Mediterranean sea level trends from 14 years of altimetry data. Global
479 and Planetary Change, *60(3-4)*, 563-575.
480 Draper and Smith, 1981. Applied Regression Analysis, 2nd ed., John Wiley and Sons.
481 Fenoglio-Marc, L.. 2002. Long-term sea level change in the Mediterranean Sea from
482 multi-satellite altimetry and tide gauges, Physics and Chemistry of the Earth, *27*,
483 1419-1431.
484 Fukumori, I., Menemenlis, D. and Lee, T., 2007. A near-uniform basin-wide sea level
485 fluctuation of the Mediterranean Sea. J. Phys. Oceanogr., *37*, 338–358.
486 García- García, D., Chao, B. F. and Boy, J.- P., 2010. Steric and mass- induced sea level
487 variations in the Mediterranean Sea revisited, J. Geophys. Res., 115, C12016,
488 doi:10.1029/2009JC005928.
489 Hurrell, J.W. 1995. Decadal trends in the North Atlantic Oscillation: regional
490 temperatures and precipitation. Science, *269*, 676–679.
491 Larnicol, G. , Ayoub, N. and Le Traon, P.Y., 2002. Major changes in Mediterranean
492 Sea level variability from 7 years of TOPEX/Poseidon and ERS-1/2 data. J. Mar.
493 Sys. 33– 34, 63–89.
494 Le Traon, P.Y. and Gauzelin, P., 1997. Response of the Mediterranean sea level to
495 atmospheric pressure forcing. Journal of Geophysical Research, *102*, 973–984.

Leuliette E.W., Nerem R. S. and Mitchum, G. T., 2004. Results of TOPEX/Poseidon and Jason-1 Calibration to Construct a Continuous Record of Mean Sea Level, Marine Geodesy, *27*, 79-94.

Millot C. and Taupier-Letage, I., 2005. Circulation in the Mediterranean Sea. In: A. Saliot (ed.) The Handbook of Environmental Chemistry, *5 (K)*, pp. 29-66.

Montogomery, D. C., Peck, V, and Vining G. G. , 2006. Introduction to Linear Regression Analysis, Wiley-Interscience.

Neter, J., Wasserman, W. and Kutner, M.H., 1989. Applied Linear Models, Boston: Irwin.

Pujol, M.I. and Larnicol, G., 2005. Mediterranean sea eddy kinetic energy variability from 11 years of altimetric data, Journal of Marine Systems, *58*, Issues 3-4, 121-142.

Roussenov, V., Stanev, E., Artale, V. and Pinardi, N., 1995. A seasonal model of the Mediterranean Sea. Journal of Geophysical Research, 100(C7):13515-13538.

Stammer, D., 1997. Global Characteristics of Ocean Variability Estimated from Regional TOPEX/POSEIDON Altimeter Measurements, Journal of Physical Oceanography, *27*, 1743-1768.

Stammer, D., Wunsch, C., Fukumori, I. and Marshall, J., 2002. State estimation in modern oceanographic research. Eos, Trans. Amer. Geophys. Union, *83*, 289, 294–295.

Tsimplis, M.N. and Josey, S.A., 2001. Forcing of the Mediterranean Sea by atmospheric oscillations over the North Atlantic. Geophysical Research Letters, *28 (5)*, 803–806.

Tsimplis M.N. and Shaw, A.G.P., 2008. The forcing of mean sea level variability around Europe, Global and Planetary Change, *63*, 196–202.

520 Vigo, I., García, D., and Chao, B. F., 2005. Change of sea level trend in the
521 Mediterranean and Black seas, J. Mar. Res., *63*, 1085 – 1100.

Figure 1

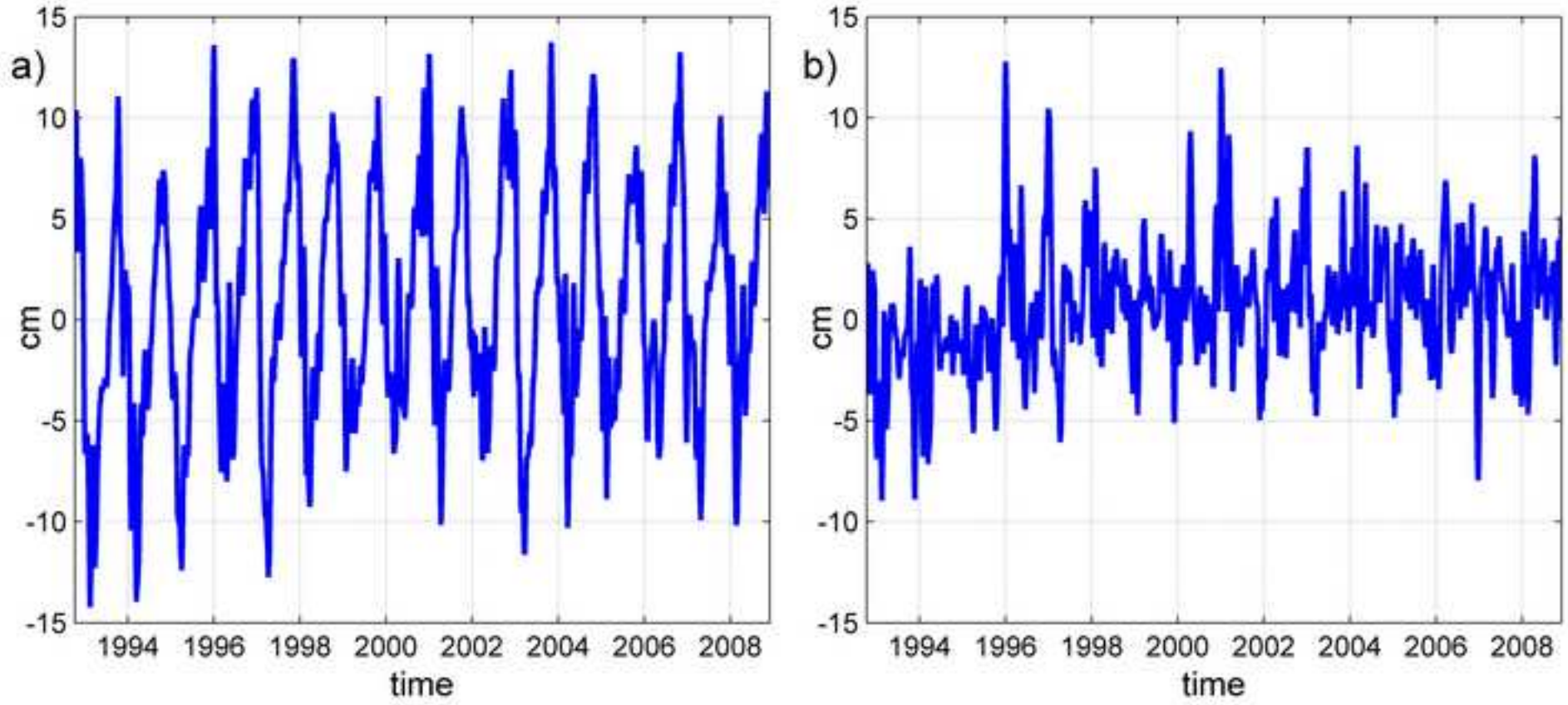
a)
b)
15
10
5
0
-5
-10
-15
cm
1994
1996
1998
2000
2002
2004
2006
2008
time

Figure 2

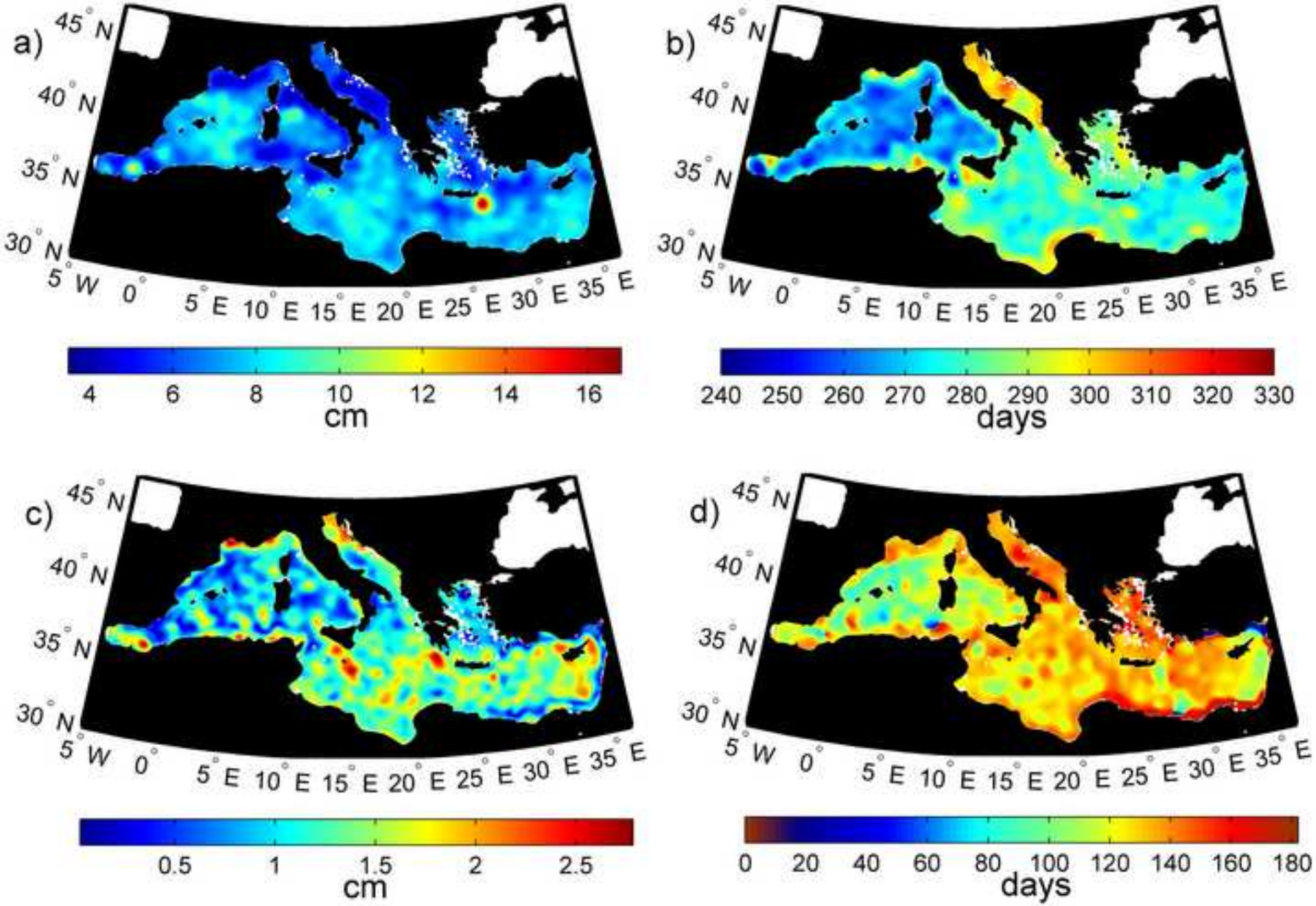
a)
45° N
40° N
35° N
30° N
5° W 0° 5° E 10° E 15° E 20° E 25° E 30° E 35° E
4 6 8 10 12 14 16
cm
b)
45° N
40° N
35° N
30° N
5° W 0° 5° E 10° E 15° E 20° E 25° E 30° E 35° E
240 250 260 270 280 290 300 310 320 330
days
c)
45° N
40° N
35° N
30° N
5° W 0° 5° E 10° E 15° E 20° E 25° E 30° E 35° E
0.5 1 1.5 2 2.5
cm
d)
45° N
40° N
35° N
30° N
5° W 0° 5° E 10° E 15° E 20° E 25° E 30° E 35° E
0 20 40 60 80 100 120 140 160 180
days

Figure 3

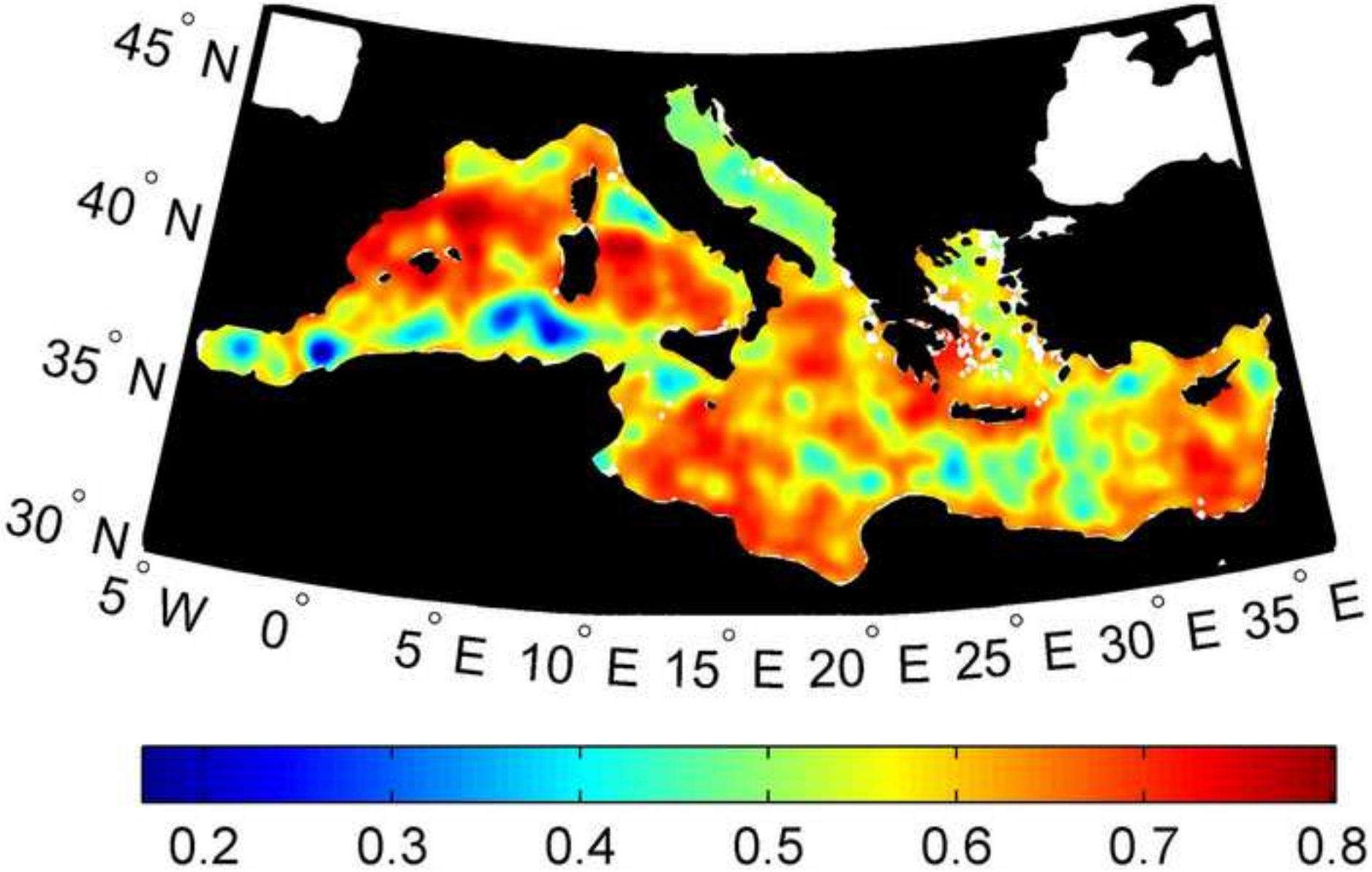

Figure 4

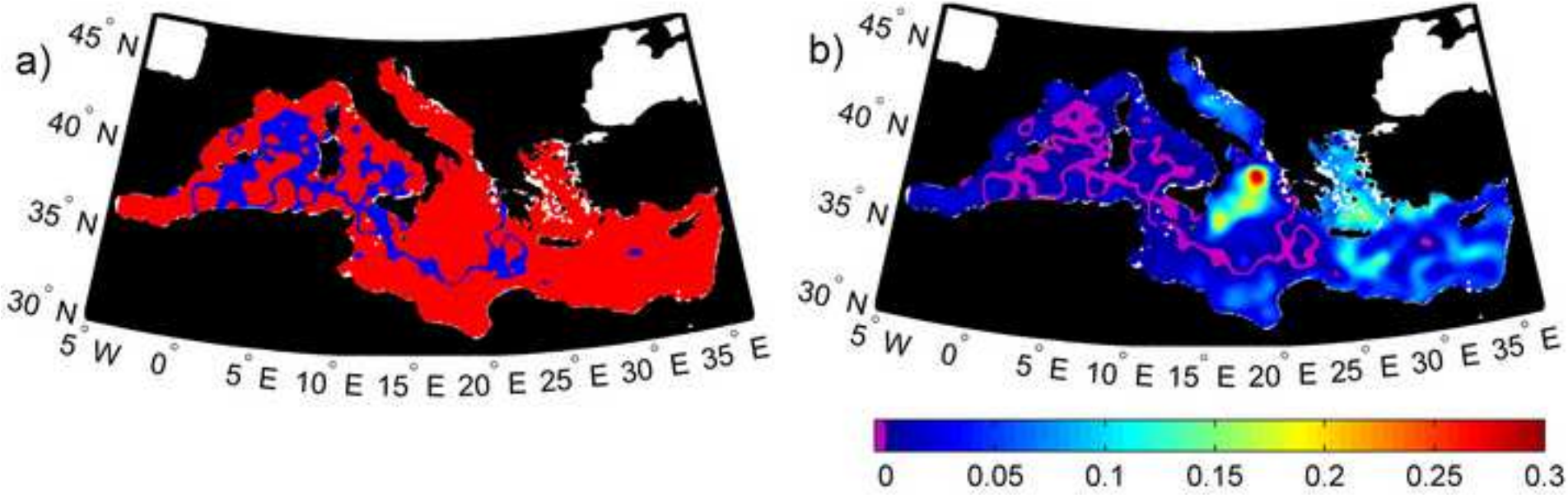

Figure 5

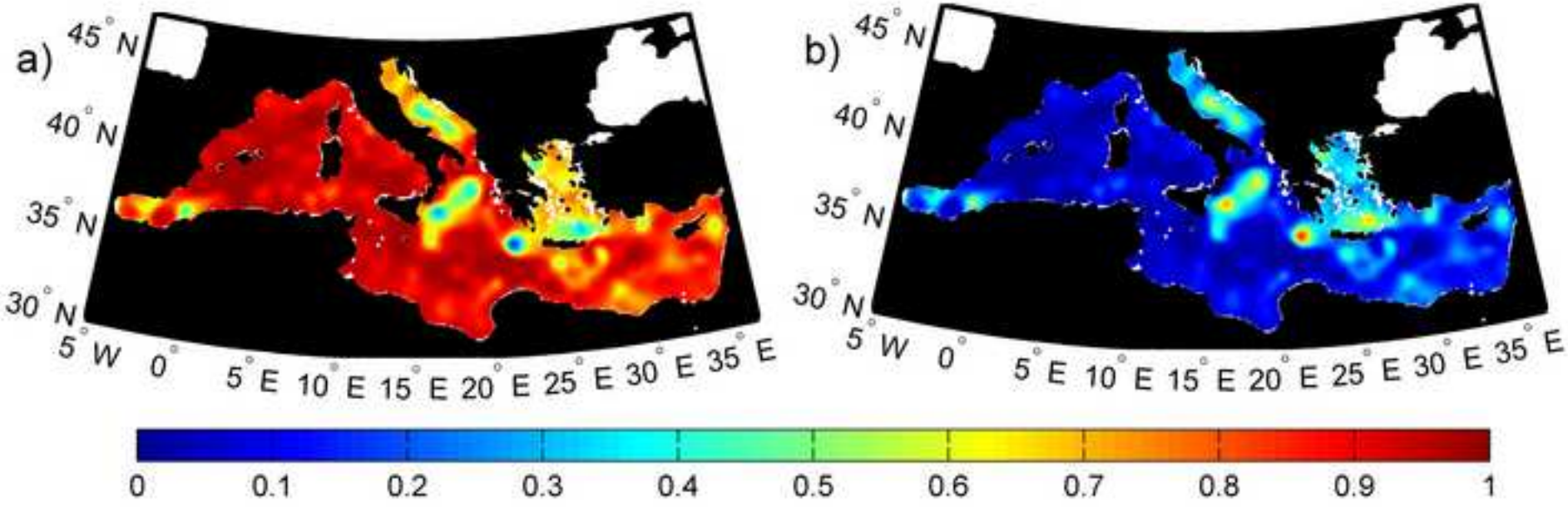

Figure 6

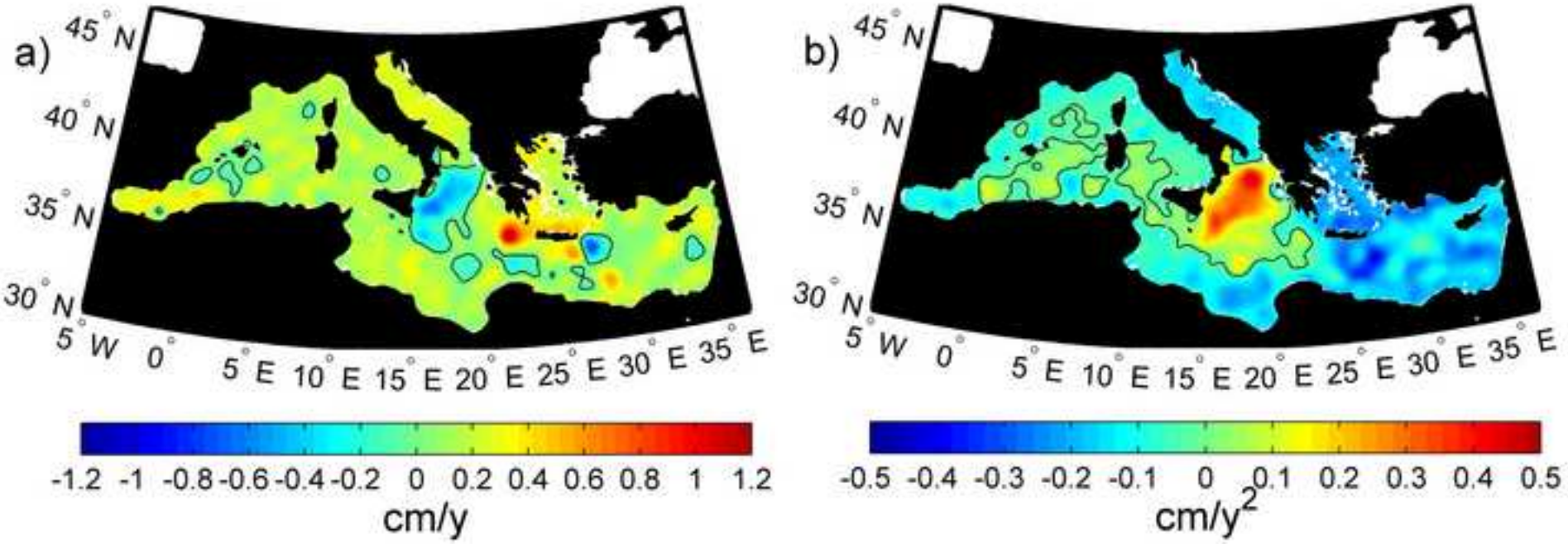

Figure 7

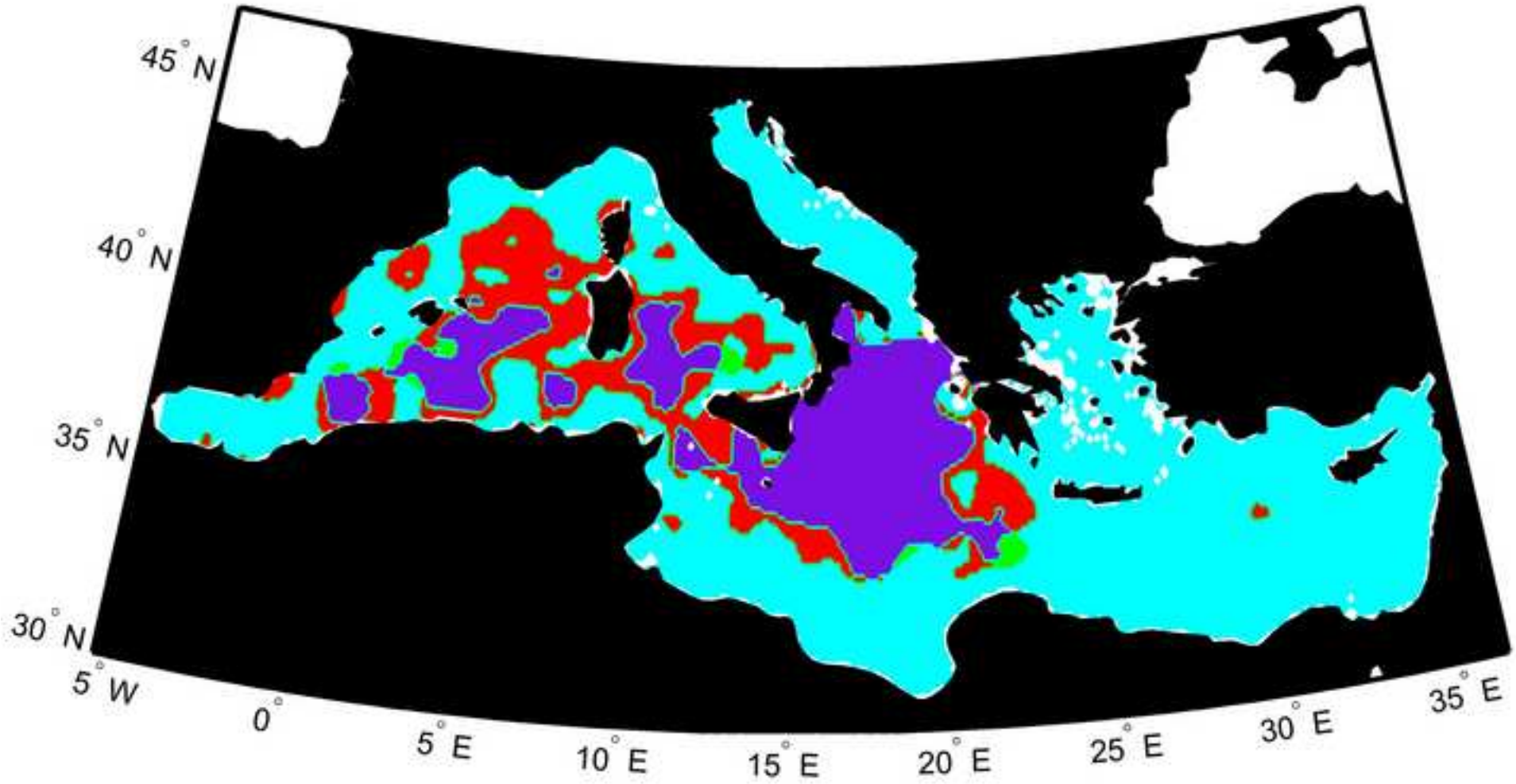

Figure 8

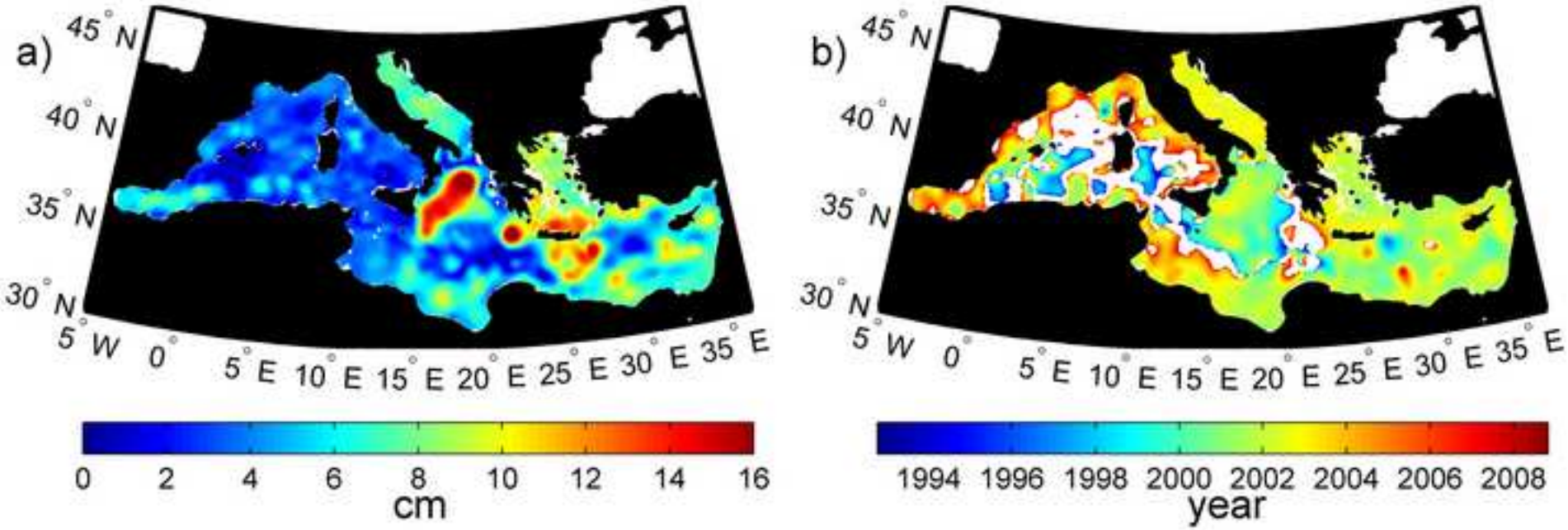
a)
45° N
40° N
35° N
30° N
5° W
0°
5° E
10° E
15° E
20° E
25° E
30° E
35° E
0
2
4
6
8
10
12
14
16
cm
b)
45° N
40° N
35° N
30° N
5° W
0°
5° E
10° E
15° E
20° E
25° E
30° E
35° E
1994
1996
1998
2000
2002
2004
2006
2008
year

Figure 9

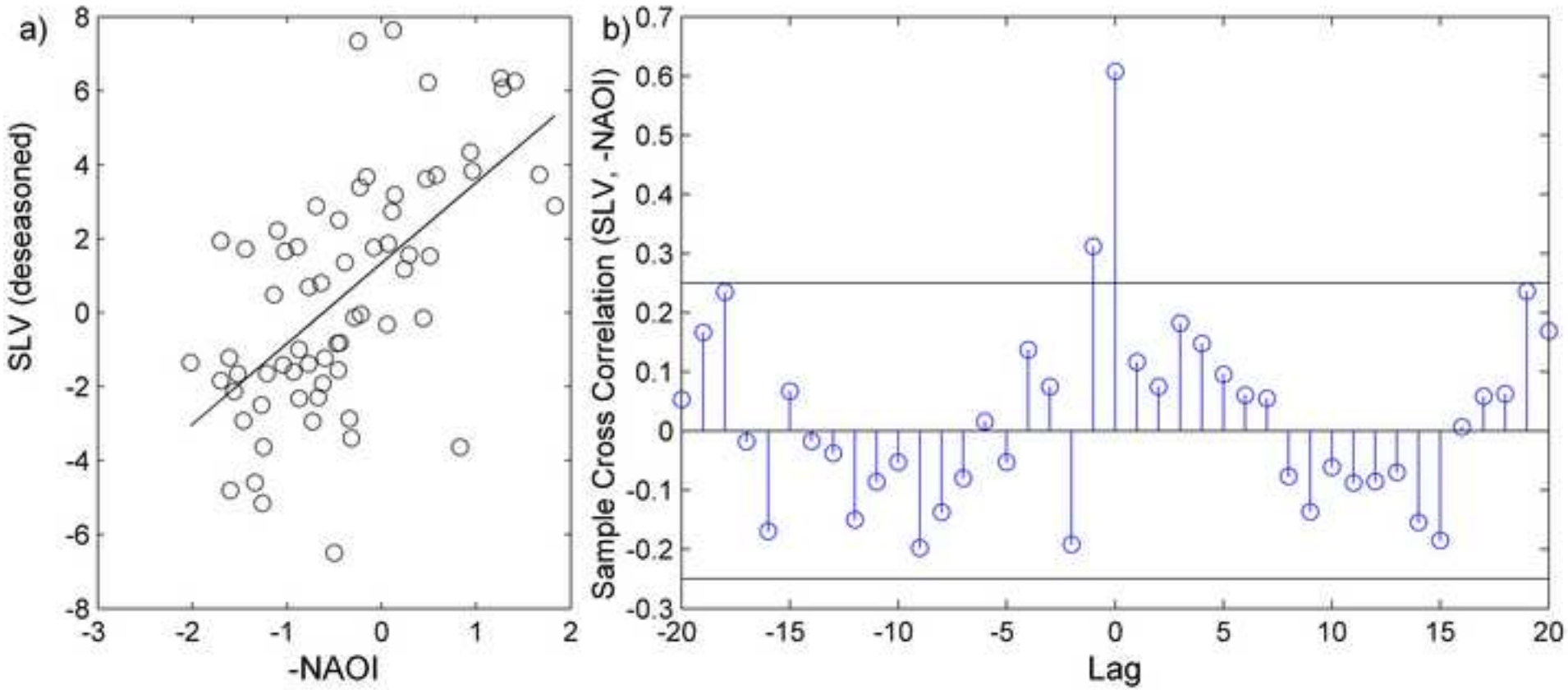
a)
SLV (deseasoned)
-NAOI
b)
Sample Cross Correlation (SLV, -NAOI)
Lag

Figure 10

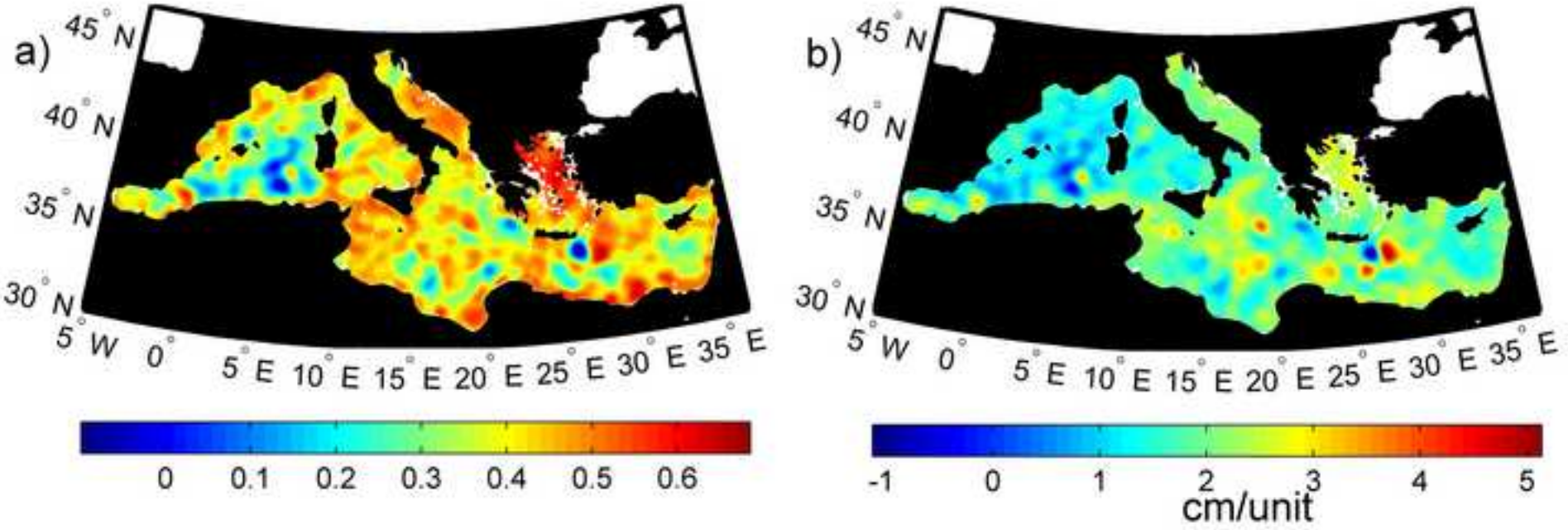

Figure 11

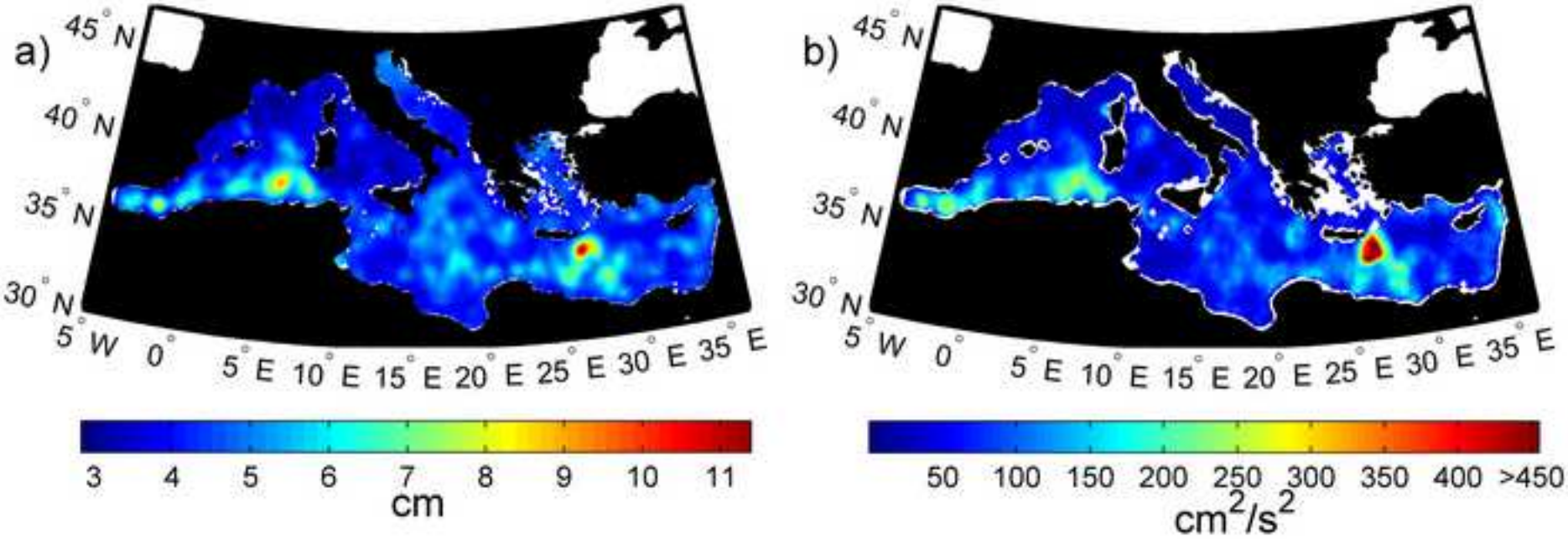
a)
45° N
40° N
35° N
30° N
5° W
0°
5° E
10° E
15° E
20° E
25° E
30° E
35° E
3
4
5
6
7
8
9
10
11
cm
b)
45° N
40° N
35° N
30° N
5° W
0°
5° E
10° E
15° E
20° E
25° E
30° E
35° E
50
100
150
200
250
300
350
400
>450
cm²/s²

Figure 12

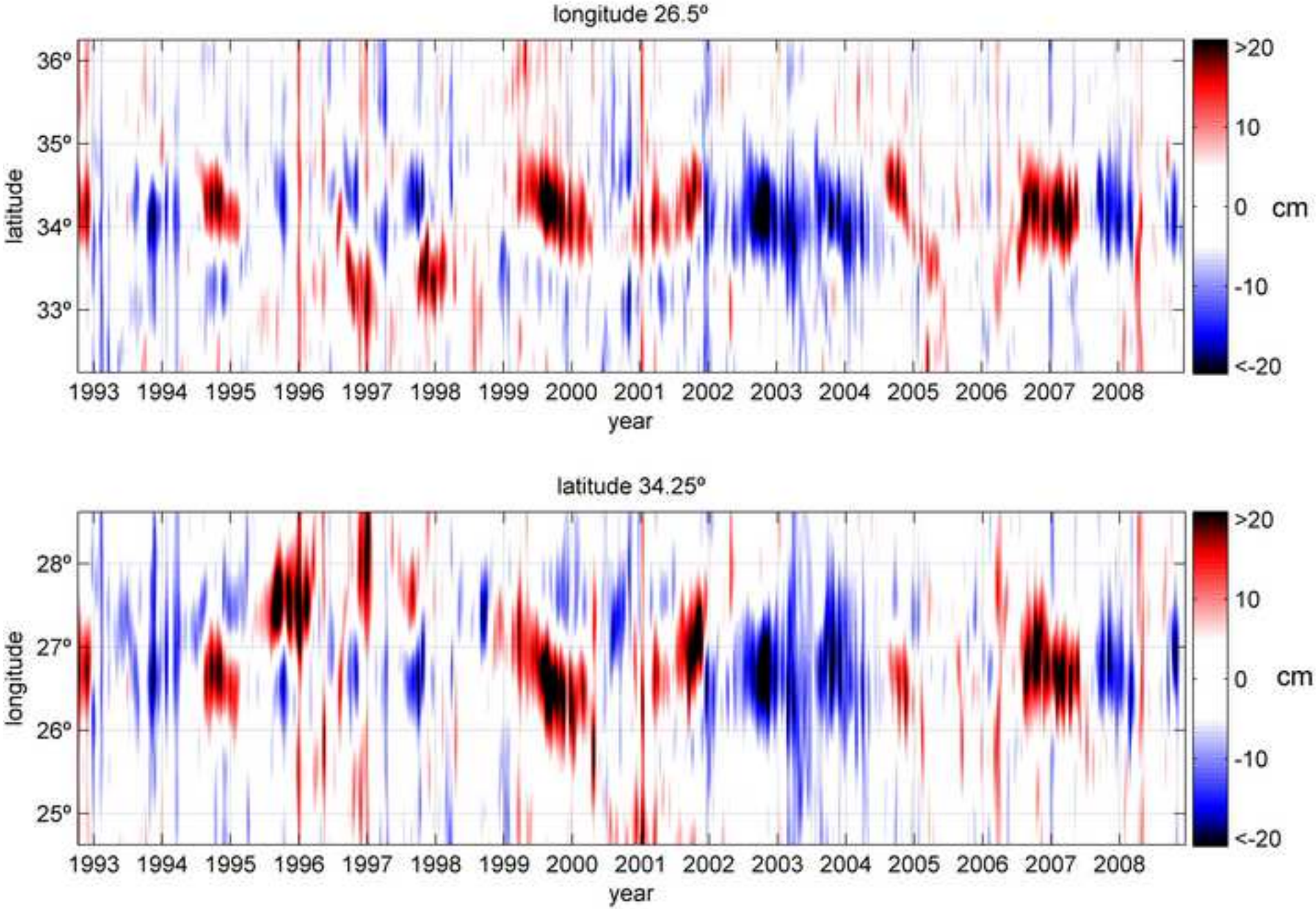
longitude 26.5°
latitude
36°
35°
34°
33°
1993 1994 1995 1996 1997 1998 1999 2000 2001 2002 2003 2004 2005 2006 2007 2008
year
>20
10
0
-10
<-20
cm
latitude 34.25°
longitude
28°
27°
26°
25°
1993 1994 1995 1996 1997 1998 1999 2000 2001 2002 2003 2004 2005 2006 2007 2008
year
>20
10
0
-10
<-20
cm

Research Highlights

- Mediterranean SLV trend over 1992-2008 is subject to a quadratic acceleration (QA).
- The QA-model outperforms existing modeling based on linear trend
- The residual low frequency SLV is driven by NAO in wintertime.
- The residual high-frequency signal variability is explained by mesoscale phenomena.